Thoracic high resolution CT using the modified VetMousetrap (TM) device is a feasible method for diagnosing canine idiopathic pulmonary fibrosis in awake West Highland White Terriers

Holopainen, Saila

2019-09

Holopainen , S , Rautala , E , Lilja-Maula , L , Lohi , H , Rajamaki , M M & Lappalainen , A K 2019 , ' Thoracic high resolution CT using the modified VetMousetrap (TM) device is a feasible method for diagnosing canine idiopathic pulmonary fibrosis in awake West Highland White Terriers ' , Veterinary Radiology & Ultrasound , vol. 60 , no. 5 , pp. 525-532 . https://doi.org/10.1111/vru.12779

http://hdl.handle.net/10138/326530
https://doi.org/10.1111/vru.12779

unspecified
acceptedVersion

Veterinary Radiology & Ultrasound

Thoracic high resolution computed tomography in awake West Highland white terriers with canine idiopathic pulmonary fibrosis using VetMousetrap™ device

Journal:	*Veterinary Radiology & Ultrasound*
Manuscript ID	VRU-04-18-085
Manuscript Type:	Original Investigation
Keywords:	dog, respiratory, position device, advanced imaging

Thoracic high resolution computed tomography in awake West Highland white terriers with canine idiopathic pulmonary fibrosis using VetMousetrap™ device

Abstract

Canine idiopathic pulmonary fibrosis (CIPF) is a chronic, progressive interstitial lung disease particularly prevalent in West Highland white terriers (WHWTs). In the present prospective study, we evaluated the feasibility of modified VetMousetrap™ device in high resolution computed tomography (HRCT) to detect CIPF in WHWTs. Twelve awake WHWTs with CIPF and 24 age matched clinically healthy control WHWTs were scanned using a helical dual slice scanner without or with minimal chemical restraint. Three evaluators blindly assessed the images for image quality and the presence of CIPF related imaging findings such as ground glass opacity (GGO). Additionally, the attenuation of the lung was quantified with ImageJ software using histogram analysis of density over the lung fields.

CT was successfully completed and the motion artefact ranked barely noticeable to mild in all dogs. The agreement between HRCT imaging findings and clinical affection status was very good with overall κ value 0.91 and percentage of agreement (PA) of 94%. There was also a very good intraobserver (κ_{range} = 0.79 - 0.91) and interobserver agreement (κ = 0.94). Moderate to severe GGO was present in all dogs with CIPF. In the ImageJ analysis a significant difference in the lung attenuation between the study groups was observed. We conclude that modified VetMousetrap™ device is applicable in diagnosing CIPF in awake WHWTs without the need of chemical restraint avoiding the anesthetic risk in these often severely hypoxic patients.

Introduction

Idiopathic pulmonary fibrosis (IPF) is an incurable interstitial lung disease that occurs both in dogs and in humans.[1,2,3,4] In dogs, the disease appears to be breed-specific, seen particularly in middle aged to older West Highland white terriers (WHWTs). [1,2,3,5] As the disease develops slowly and the clinical signs can be confused with other respiratory or cardiac diseases as well as with normal ageing process, the diagnosis can be challenging to achieve. In humans, the presence of usual interstitial pneumonia (UIP) pattern in high resolution computed tomography (HRCT) images is the golden standard for diagnosis of IPF and lung biopsies are only needed if HRCT is inconclusive.[4] In dogs, definite diagnosis of canine IPF (CIPF) requires histopathological examination of lung tissue and due to invasiveness of lung biopsies, the diagnosis is often confirmed at necropsy.[6] HRCT has been shown to be a reliable and useful diagnostic tool also in CIPF.[3,7,8,9] However, the technique used has required general anesthesia, which in these respiratory compromised patients might be risky. Recently, HRCT imaging findings under general anesthesia and sedation were compared.[10]

A transparent positioning device, VetMousetrap™ has been designed to enable CT scanning in awake animals.[11] It was first used in CT imaging of thorax of awake healthy cats and cats with different thoracic diseases.[11,12] CT imaging with minimal or no sedation has been described also in dogs with respiratory and abdominal diseases.[13,14,15] The positioning device could provide a rapid and safe alternative to obtain thoracic CT without need for sedation or general anesthesia.

Quantitative computer image analysis approaches, such as ImageJ, have been applied to detect lung pathology in humans.[16,17] ImageJ is a Java-based open access imaging software used for many biomedical imaging applications and allows the quantitative assessment of the

DICOM images over the whole lung area.[18] This could provide more accurate reflection of diffuse interstitial lung diseases and superior assessment of the severity of the disease when compared to conventional techniques.

The objective of the present prospective study was to evaluate the feasibility of CT studies in diagnosing CIPF in WHWTs using only physical restraint. The hypothesis was that thoracic HRCT imaging of awake animals using modified VetMousetrap™ device could be performed to obtain acceptable image quality. In addition, we analysed the attenuation of the entire lung fields of the dogs with the ImageJ software and hypothetized increased attenuation in CIPF dogs when compared to controls.

Materials and methods

All the WHWTs were privately owned and prospectively recruited. The study protocols were approved by the "Animal Ethics Committee at the State Provincial Office" (permit number 7383/04.10.07/2013, date of approval: 13 November 2013).

The study group consisted of 12 CIPF and 24 healthy age matched WHWTs. The median age of the WHWTs with CIPF (8 males, 4 females) was 12.8 (range 8-14) years and for the clinically healthy controls (10 males, 14 females) 11.2 (range 7-14) years. The clinical status was based on clinical signs, physical examination findings, hematological and serum biochemical analysis, measurement of C-reactive protein, thoracic radiography and arterial blood gas analysis in all dogs. In addition, for 14/36 fecal analysis, 28/36 6-minute walk test, 12/36 echocardiography and 4/36 dogs bronchoscopy and bronchoalveolar lavage (BAL) was performed. The tentative diagnosis of CIPF was based on previously described findings in WHWTs with CIPF, including typical auscultation findings, low partial pressure of arterial

oxygen (PaO_2) values and exclusion of other cardiac and respiratory diseases.[3] The mean PaO_2 for the CIPF dogs was 60.7 mmHg (range 49.4-69.1 mmHg) and for the control group 96.1 mmHg (range 86.1-107.0 mmHg). The control WHWTs had no signs or findings of any respiratory disease. Eight of 12 dogs with CIPF died or were euthanized before the study endpoint in October 2015 and histopathological confirmation of CIPF was done from lung tissue biopsies. One healthy WHWT was euthanized due to neurological signs and was diagnosed with brain astrocytoma. As the aim of this study was to evaluate the use of modified VetMousetrap™ in detecting CIPF, patients with suspicion of other respiratory diseases, such as pneumonia or lung neoplasia, were excluded from the study.

Thoracic HRCT was performed using a helical dual slice scanner (Somatom Emotion Duo, Siemens AG, Forchheim, Germany) and modified VetMousetrap™ (Universal Medical Systems, Inc. Cleveland, Ohio, USA) device without anesthesia between August 2014 and February 2015. For CT scanning the dogs were positioned in sternal recumbency on the VetMousetrap™ device and instead of a lid, velcro tapes and foam cushions were used to fix the dog comfortably into the box and to prevent motion. To relieve anxiety, four WHWTs were given butorphanol (Zoetis) 0.2 mg/kg intramuscularly 15 minutes before scanning. Axial HRCT protocol with high spatial resolution image reconstruction algorithm was employed using 1 mm slice thickness with 7.5 mm table movement, 130 kV and 100 mAs, and matrix of 512 x 512. Tube rotation time was 0.8 s.

HRCT image sets were randomized, anonymized and reviewed by three evaluators. Each observer independently evaluated images three times with minimum of one week interval. Two evaluators were veterinary radiologists and one was a veterinary practitioner. The images were viewed using OsiriX imaging software (Pixmeo, Geneva, Switzerland) and reviewed with pulmonary window settings (WL -500, WW 1500). Affection status of each animal was

recorded as healthy or CIPF. Left and right cranial, middle and caudal lung fields were separately assessed for presence of ground glass opacity (GGO).[3,8] The cranial zone was defined as cranial to the bifurcation, the middle zone as five slices caudal to the bifurcation and the caudal zone as caudal to these. The presence of GGO was determined in each of the six zones by the three observers and the extent was scored as mild if present only in one zone, moderate if present in two or three zones and severe if present in four zones or more. Motion artefact was characterized by blurriness of one or more areas of lung fields and loss of sharp edges of pulmonary vessels and airway walls. The image quality for every lung field from the most representative slice was evaluated separately using criteria that addressed the presence of motion artefact as shown in Table 1.

Quantitative CT values in Hounsfield units (HU) of the lung fields were measured using Fiji ImageJ 1.50b software by primary author to objectively estimate the attenuation of the lung. For all the lung zones three slices were selected and anatomical lung outlines of each of the lung segments of both the left and right lung were depicted as regions of interest (ROI) (Figure 1). The pixel values were measured representing the average global attenuation value of the ROIs as HUs.

Descriptive statistics are presented as mean ± standard deviation (SD) and 95% confidence interval for mean or percentages for continuous and normally distributed variables as median and range for noncontinuous variables. For quantitative analysis, normality of the data distribution was tested with the use of the Kolmogorov–Smirnoff and Shapiro-Wilk –tests. For affection status, the agreement between clinical and CT findings was evaluated by Cohen's kappa (κ) statistics and percentage of agreement (PA). Intra- and interobserver variabilities were analysed using κ statistics. Agreement was classified as “very good” (κ>0.8), “good” (κ=0.61–0.8), “moderate” (κ=0.41–0.6), “fair” (κ=0.21–0.4), or “poor” ($\kappa \leqslant$

0.2).[19] To describe the certainty of the coefficient, 95% confidence intervals for the κ coefficients were computed.

To assess CT imaging findings and motion artefacts, frequency tables were computed by lung field and observer. Between the three observation rounds the mode value was chosen or in case every result was different, the median was chosen, first for every rater over lung fields, and finally over raters to obtain the overall score. The motion artefacts and attenuation between the two study groups were compared by the use of Student's *t*-test. To compare the lung fields a cumulative logistic regression model was fitted and the probability of higher values for motion artefact was modelled using area as a fixed effect in the model and dog and rater as random effects. Data was analysed with commercially available software SAS® System for Windows, version 9.2 (SAS Institute Inc., Cary, NC, USA). P-values, describing the difference from zero, were calculated. Values of $P < 0.05$ were considered significant.

Results

The agreement between HRCT imaging findings and clinical affection status was very good with overall κ value of all observers and all rounds being 0.91 ($P < 0.0001$). κ values varied from 0.61 to 1.00. The mean overall PA was 94% (range 83% -100%). With observer 1 the most disagreement with clinical data and the HRCT imaging results was found with the first round, with observer 2 with the third round and with observer 3 with the second and third round (Table 2).

The κ values for intraobserver agreement were very good, except in one case where the κ value was 0.79 (good), in diagnosing CIPF between the observation rounds for all observers (Table 3). As for overall interobserver agreement, κ values indicated a very good agreement

between the observers. When the most common interpretation per observation for each observer was chosen, the overall interobserver agreement was $\kappa = 0.94$ ($P < 0.0001$). Two of the raters (observers 2 and 3) resulted to a complete agreement and agreement with the third rater (observer 1) was found very good ($\kappa = 0.86$) when interobserver agreement between pairs of observers was calculated (Table 4).

Motion artefact was found none to mild in all images chosen for evaluation. No significant difference was found in the motion artefact between different lung fields ($P = 0.71$) or between the two study groups ($P = 0.97$).

Moderate (1/12) to severe (11/12) GGO was detected in all CIPF dogs. In all 12 CIPF dogs the abnormalities seen on HRCT were patchily distributed over the lung area. In 6/24 clinically healthy WHWTs mild and in one clinically healthy WHWT moderate GGO was observed. A parenchymal band was detected in the right cranial lobe of one control dog. Other CT findings were not detected in the controls. Examples of HRCT images obtained are illustrated in Figures 2 and 3.

ImageJ analysis showed a significant difference in mean lung attenuation between the two study groups. In quantitative analysis the HU values of lung fields were significantly higher in CIPF dogs when compared with controls (group mean ± SD: healthy dogs -708 ± 55.8 HU, 95% confidence interval for mean -732 to -685 HU; CIPF dogs -495 ± 66.8 HU, 95% confidence interval for mean: -538 to -453 HU, $P < 0.0005$).

All dogs were cooperative during scanning. Patient preparation time was less than 5 minutes. No complications were noticed.

Discussion

The aim of the present study was to evaluate the feasibility of modified VetMousetrap™ device in HRCT scanning in detecting CIPF in WHWTs. In the absence of lung biopsies, thoracic HRCT is an important diagnostic tool for diagnosis of CIPF.[6] However, general anesthesia is usually required to obtain thoracic HRCT scans in animals and CIPF dogs commonly have substantial hypoxemia possessing an increased anesthetic risk.[3] The positioning device enabling thoracic CT imaging without general anesthesia or sedation, such as VetMousetrap™ could offer a rapid and safe alternative. In our study, we used no or minimal sedation during scanning. The four dogs receiving butorphanol all remained fully conscious and ambulatory.

In human pediatric radiology, HRCT scanning is often performed without general anesthesia.[20] In previous studies where VetMousetrap™ device has been used to scan awake or mildly sedated animals, image quality has been adequate for diagnosis of airway diseases including dogs with primary laryngeal and tracheal airway obstruction,[13] pulmonary thromboembolism,[15] cats with upper airway obstruction and allergic asthma,[21-23] and dogs with abdominal diseases and traumatic pelvic fractures.[14,24] Motion artefact has been considered absent or mild in majority of examinations,[11,12,14] as was the case also in our study. Image quality was considered adequate for diagnosis in spite of the scan acquisition with the animals awake and without a respiratory pause.

The patient movement and respiratory motion in awake animals during scanning can cause artefacts which impair the image quality. However, motion artefacts can be minimized with the patient immobilization and imaging techniques. Fastest available gantry rotation time is

used to reduce the scanning time. Multidetector-row spiral scanners (MDCT) would be optimal for the method in question as they allow even shorter scanning times and less motion artefact.[25] Spiral scanning with MDCT would allow complete visualization of all parts of the lungs and enable the generation of multiplanar reformation images. In our study, no statistically significant differences in motion artefact were identified between cranial, middle and caudal parts of the lung. Moreover, scanning under general anesthesia often causes varying degrees of hypostatic congestion and dependent atelectasis which may mimic pathological changes eliciting the need for additional scans in different postures.[26,27]

Correlation between the clinical workup and CT diagnosis was high with overall κ value 0.91 and PA 94%. The κ value range is 0–1, with 0 indicating only chance agreement and 1 perfect agreement.[28] The diagnostic accuracy obtained is consistent with previous studies of thoracic CT in anesthetized dogs.[8,29] In humans, HRCT performs well in diagnosing UIP using histopathology as the reference standard with an accuracy of 80% to 90% when UIP is the first diagnosis based on imaging findings.[30-32] Both intra- and interobserver agreements were also very good in our study. In human studies inter-observer agreement for the diagnosis of IPF has been fair to moderate.[33,34] However, in these studies the different interstitial lung disease patterns were evaluated separately which makes accuracy of diagnosis more challenging. In our study, the study design (observers knew that the dogs were either clinically healthy or had IPF) could have had an effect on good correlation between clinical workup and CT diagnosis and also between intra- and interobserver agreement.

Moderate to severe GGO, which has previously been described as the hallmark of the CIPF,[3,7,8] was present in all of the dogs with CIPF. The differences between thoracic HRCT imaging findings for CIPF under general anesthesia and sedation have been recently described

stating that different information in terms of extent of GGO and grading of mosaic pattern may be observed between the two methods.[10] Inability to obtain images during specific respiration phase may cause secondary artefactual changes for example due to underinflation of the lungs during expiration,[8] and motion artefacts could potentially influence on the estimations of these parenchymal lesions. In our study, especially in the most caudal images near the diaphragm, severe motion artefact was common. However, in every case at least one image was representative and diagnosis of GGO was possible. Because of the possible influence of the motion artefacts, we did not evaluate the images for more local abnormalities such as parenchymal bands and subpleural thickening. In a recent study it was demonstrated that identification of this kind of lesions did not differ between acquisition of thoracic HRCT under general anesthesia and sedation.[10]

With ImageJ software, histogram analysis of density in pixels can be performed to differentiate normal and fibrotic lung parenchyma. ImageJ CT image analysis was able to quantify the difference in attenuation over the lung fields between CIPF and healthy WHWTs and detect distinctly CIPF from healthy dogs. In our study the HU values of both healthy and CIPF dogs were higher than in the previous studies where the difference in the lung attenuation of CIPF and healthy WHWTs under general anesthesia were assessed.[3,9] This could be due to mechanical inflation of the lungs under general anesthesia. Another possible cause might have been inclusion of fat or other tissues than lung tissue in the ROIs, which could be overcome by adding upper HU limit to CT number range but was not implemented as severe pulmonary changes could be missed.[35] Since in IPF mosaic pattern with patchily distributed high-attenuation areas is often recognized.[36] ImageJ analysis could provide more objective evaluation of the overall lung attenuation. This computer image analysis approach

has potential in the assessment of canine interstitial lung diseases for clinical and research purposes.

Imaging without anesthesia appeared acceptable to the owners as all approved CT imaging without chemical restraint. Some owners refused conventional HRCT under general anesthesia, but agreed thoracic HRCT study using modified VetMousetrap™ device.

Limitations of this study include relatively small number of dogs and lack of histopathological confirmation of affection status for all of the dogs. However, histopathology was available in majority of diseased WHWTs and pathological results verified diagnosis achieved by HRCT. In six clinically healthy control dogs there was mild and in one moderate GGO in HRCT images. These patients were free of respiratory signs and had normal oxygen level in arterial blood. In these patients, follow-up examinations with CT imaging would be recommended to evaluate if these changes represent the early signs of CIPF. Although our study was performed with a dual slice scanner the results for detecting CIPF was good. MDCT scanners that are faster and have more detectors are widely available for clinical use and they could be used to find more subtle changes.

In conclusion, CT imaging with modified VetMousetrap™ device was feasible in diagnosing CIPF in awake WHWTs without the need of chemical restraint. Since anesthesia and sedation is often avoided in these often severely hypoxic patients in order to prevent further respiratory compromise, this would provide a valuable alternative in the clinical setting. Image quality was adequate for assessment of the existence of the disease with very good intra- and interobserver accuracy. Quantitative computer image approaches such as ImageJ analysis could be applicable in assessment of CIPF.

272

273

References

1. Corcoran B, Cobb M, Martin M, Dukes-McEwan J, French A. Chronic pulmonary disease in West Highland White Terriers. *Vet Rec*. 1999;144:611–616.

2. Lobetti RG, Milner R, Lane E. Chronic idiopathic pulmonary fibrosis in five dogs. *J Am Anim Hosp Assoc*. 2001;37:119–27.

3. Heikkilä H, Lappalainen A, Day M, Clercx C, Rajamäki M. Clinical, bronchoscopic, histopathologic, diagnostic imaging, and arterial oxygenation findings in West Highland White Terriers with idiopathic pulmonary fibrosis. *J Vet Intern Med*. 2011;25:433–9.

4. Raghu G, Collard HR, Egan JJ, Martinez FJ, Behr J, Brown KK, et al. An official ATS/ERS/JRS/ALAT statement: idiopathic pulmonary fibrosis: evidence-based guidelines for diagnosis and management. *Am J Resp Crit Care Med*. 2011;183:788–824.

5. Norris AJ, Naydan DK, Wilson DW. Interstitial lung disease in West Highland White Terriers. *Vet Pathol*. 2005;42:35–41.

6. Heikkilä-Laurila HP, Rajamäki MM. Idiopathic pulmonary fibrosis in West Highland white terriers. *Vet Clin N Am Small Anim Pract*. 2014;44:129–42.

7. Corcoran BM, King LG, Schwarz T, Hammond G, Sullivan M. Further characterisation of the clinical features of chronic pulmonary disease in West Highland white terriers. *Vet Rec*. 2011;168:354–355.

8. Johnson V, Corcoran B, Wotton P, Schwarz T, Sullivan M. Thoracic high‐resolution computed tomographic findings in dogs with canine idiopathic pulmonary fibrosis. *J Small Anim Pract*. 2005;46:381–8.

9. Thierry F, Handel I, Hammond G, King LG, Corcoran BM, Schwarz T. Further characterization of computed tomographic and clinical features for staging and prognosis of idiopathic pulmonary fibrosis in West Highland white terriers. *Vet Radiol Ultrasound*. 2017;00:1–8.

10. Roels E, Couvreur T, Farnir F, Clercx C, Verschakelen J, Bolen G. Comparison between sedation and general anesthesia for high resolution computed tomographic characterization of canine idiopathic pulmonary fibrosis in west highland white terriers. *Vet Radiol Ultrasound*. 2017;58:284–294.

11. Oliveira CR, Mitchell MA, O'Brien RT. Thoracic computed tomography in feline patients without use of chemical restraint. *Vet Radiol Ultrasound*. 2011;52:368–76.

12. Oliveira CR, Ranallo FN, Pijanowski GJ, Mitchell MA, O'Brien MA, McMichael M, et al. The Vetmousetrap™: a device for computed tomographic imaging of the thorax of awake cats. *Vet Radiol Ultrasound*. 2011;52:41–52.

13. Stadler K, Hartman S, Matheson J, O'Brien R. Computed tomographic imaging of dogs with primary laryngeal or tracheal airway obstruction. *Vet Radiol Ultrasound*. 2011;52:377–84.

14. Shanaman MM, Hartman SK, O'Brien RT. Feasibility for using dual‐phase contrast‐enhanced multi‐detector helical computed tomography to evaluate awake and sedated dogs with acute abdominal signs. *Vet Radiol Ultrasound*. 2012;53:605–12.

15. Ngwenyama TR, Herring JM, O'Brien M, Hartman SK, Galloway KA, O'Brien RT. Contrast‐enhanced multidetector computed tomography to diagnose pulmonary thromboembolism in an awake dog with pyothorax. *J Vet Emerg Crit Care*. 2014;24:731–8.

16. Erdal BS, Crouser ED, Yildiz V, King MA, Patterson AT, Knopp MV, et al. Quantitative computerized two-point correlation analysis of lung CT scans correlates with pulmonary function in pulmonary sarcoidosis. *Chest.* 2012;142:1589–97.

17. Park SC, Tan J, Wang X, Lederman D, Leader JK, Kim SH, et al. Computer-aided detection of early interstitial lung diseases using low-dose CT images. *Phys Med Biol*. 2011;56:1139.

18. Abràmoff MD, Magalhães PJ, Ram SJ. Image processing with ImageJ. *Biophoton Int*. 2004;11:36–42.

19. Landis JR, Koch GG. The measurement of observer agreement for categorical data. *Biometrics*. 1977;33:159–74.

20. Garcia-Peña P, Lucaya J. HRCT in children: technique and indications. *Eur Radiol Suppl*. 2004;14:13–30.

21. Stadler K, O'Brien R. Computed tomography of nonanesthetized cats with upper airway obstruction. *Vet Radiol Ultrasound*. 2013;54:231–6.

22. Trzil JE, Reinero CR. Update on feline asthma. *Vet Clin N Am Small Anim Pract*. 2014;44:91–105.

23. Masseau I, Banuelos A, Dodam J, Cohn LA, Reinero C. Comparison of lung attenuation and heterogeneity between cats with experimentally induced allergic asthma, naturally occurring asthma and normal cats. *Vet Radiol Ultrasound*. 2015;56:595–601.

24. Lee K, Heng HG, Jeong J, Naughton JF, Rohleder JJ. Feasibility of computed tomography in awake dogs with traumatic pelvic fracture. *Vet Radiol Ultrasound*. 2012;53:412–6.

25. Bastos Md, Lee EY, Strauss KJ, Zurakowski D, Tracy DA, Boiselle PM. Motion artifact on high-resolution CT images of pediatric patients: comparison of volumetric and axial CT methods. *Am J Roentgenol*. 2009;193:1414–8.

26. Schwarz LA, Tidwell AS. Alternative imaging of the lung. *Clin Tech Small Anim Pract*. 1999;14:187–206.

27. Staffieri F, Franchini D, Carella GL, Montanaro MG, Valentini V, Driessen B, et al. Computed tomographic analysis of the effects of two inspired oxygen concentrations on pulmonary aeration in anesthetized and mechanically ventilated dogs. *Am J Vet Res*. 2007;68:925–31.

28. Brennan P, Silman A. Statistical methods for assessing observer variability in clinical measures. *BMJ*. 19926;304:1491–4.

29. Miller J, Wallace T, Greggory T, Friedburg JS. Thoracic CT in the intensive care unit: assessment of clinical usefulness. *Radiology*. 1998; 209:491–498.

30. Hunninghake GW, Lynch DA, Galvin JR, Gross BH, Mu N, Schwartz DA, et al. Radiologic findings are strongly associated with a pathologic diagnosis of usual interstitial pneumonia. *Chest*. 2003;124:1215–23.

31. Martin MD, Chung JH, Kanne JP. Idiopathic Pulmonary Fibrosis. *J Thorac Imaging*. 2016;31:127–39.

32. Tsubamoto M, Müller NL, Johkoh T, Ichikado K, Taniguchi H, Kondoh Y, et al. Pathologic subgroups of nonspecific interstitial pneumonia: differential diagnosis from other idiopathic interstitial pneumonias on high-resolution computed tomography. *J Comput Assist Tomogr*. 2005;29:793–800.

33. Aziz ZA, Wells AU, Hansell DM, Bain GA, Copley SJ, Desai SR, et al. HRCT diagnosis of diffuse parenchymal lung disease: inter-observer variation. *Thorax*. 2004 Jun;59:506–11.

34. Thomeer M, Demedts M, Behr J, Buhl R, Costabel U, Flower CD, et al. Multidisciplinary interobserver agreement in the diagnosis of idiopathic pulmonary fibrosis. *Eur Respir J*. 2008;31:585–91.

35. McEvoy FJ, Buelund L, Strathe AB, Willesen JL, Koch J, Webster P, et al. Quantitative computed tomography evaluation of pulmonary disease. *Vet Radiol Ultrasound* 2009;50:47–51.

36. Kligerman SJ, Henry T, Lin CT, Franks TJ, Galvin JR. Mosaic attenuation: etiology, methods of differentiation, and pitfalls. *RadioGraphics* 2015;35:1360–1380.

Tables

Table 1. The score for evaluation of motion artefact

Score	Quality	Definition
1	Good	None or mild motion artefact, good/very good for interpretation
2	Moderate	Moderate motion artefact, adequate for interpretation
3	Poor	Severe motion artefact, nonacceptable for interpretation

Table 2. The agreement between high resolution computed tomography imaging findings and clinical affection status* for three observers

Observer	Round	Kappa (SD)	95% CI	p-value
Overall (1-3)	1-3	0.910 (0.096)	(0.721 - 1.000)	<.0001
1	1	0.609 (0.143)	(0.329 - 0.889)	0.0002
	2	0.800 (0.108)	(0.588 - 1.000)	<.0001
	3	0.745 (0.117)	(0.516 - 0.973)	<.0001
2	1	1.000 (0.000)	(1.000 - 1.000)	<.0001
	2	0.936 (0.063)	(0.813 - 1.000)	<.0001
	3	0.870 (0.089)	(0.695 - 1.000)	<.0001
3	1	0.936 (0.063)	(0.813 - 1.000)	<.0001
	2	0.875 (0.086)	(0.707 - 1.000)	<.0001
	3	0.875 (0.086)	(0.707 - 1.000)	<.0001

*healthy vs. diseased status based on history, clinical examination, blood samples including hematology, C-reactive protein, serum biochemistry and arterial blood gas analysis, thoracic radiographs and 6-minute walk test

Table 3. Intraobserver agreement between high resolution computed tomography imaging findings and clinical affection status in diagnosing canine idiopathic pulmonary fibrosis

Observer	Kappa (SD)	95% CI	p-value
1	0.848 (0.096)	(0.659 - 1.000)	<.0001
2	0.913 (0.096)	(0.724 - 1.000)	<.0001
3	0.792 (0.096)	(0.603 - 1.000)	<.0001

Table 4. Interobserver agreement between high resolution computed tomography imaging findings and clinical affection status in diagnosing canine idiopathic pulmonary fibrosis

Observer	Kappa (SD)	95% CI	p-value
Overall	0.936 (0.063)	(0.813 - 1.000)	<.0001
1 vs 2	0.862 (0.094)	(0.678 - 1.000)	<.0001
1 vs 3	0.862 (0.094)	(0.678 - 1.000)	<.0001
2 vs 3	1.000 (0.000)	(1.000 - 1.000)	<.0001

Figure legends

Figure 1. Measurement of lung attenuation of the left caudal field of the lung in a healthy West Highland white terrier. Regions of interest (ROI) were manually placed for cranial, middle and caudal lung areas of both lungs for the measurement of mean lung density in Hounsfield units for each ROI using Fiji ImageJ 1.50b software.

Figure 2. Transverse high resolution computed tomographic image of the middle thorax in a healthy West Highland white terrier under general anesthesia (A) and using VetMousetrap™ device (B).

Figure 3. Transverse high resolution computed tomographic image using VetMousetrap™ device of a dog with canine idiopathic pulmonary fibrosis with severe ground glass opacity.

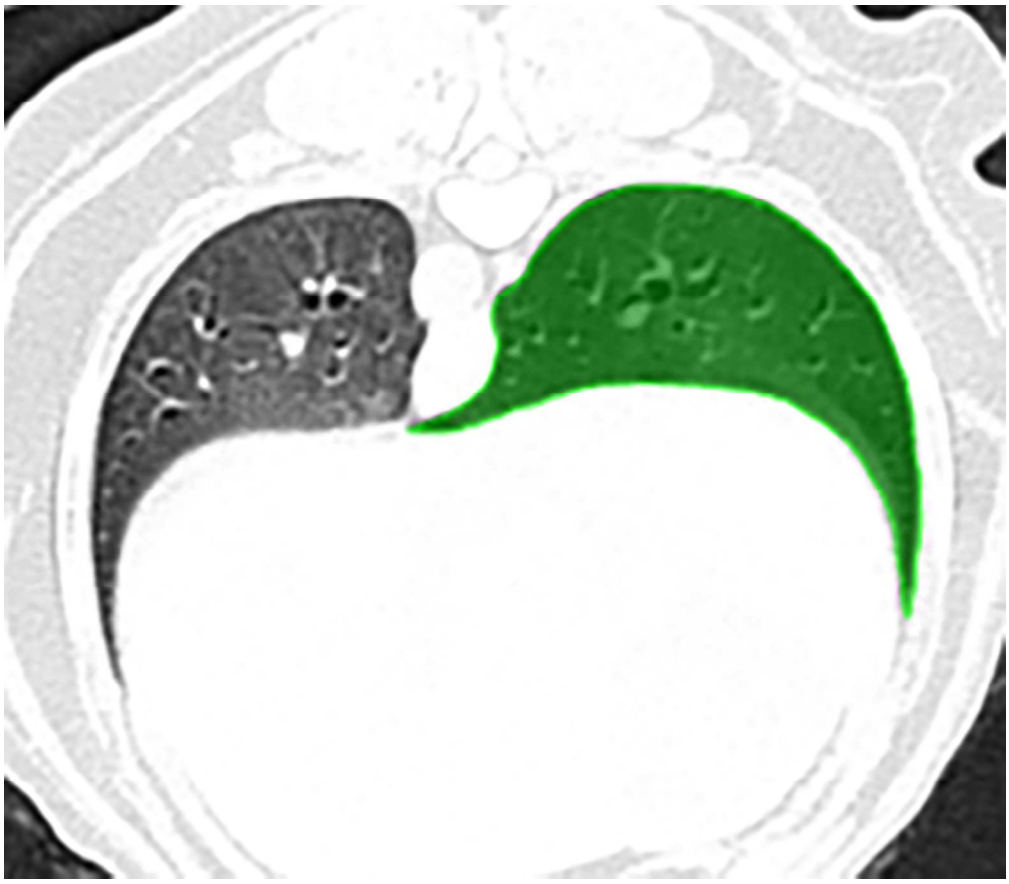

Figure 1. Measurement of lung attenuation of the left caudal field of the lung in a healthy West Highland white terrier. Regions of interest (ROI) were manually placed for cranial, middle and caudal lung areas of both lungs for the measurement of mean lung density in Hounsfield units for each ROI using Fiji ImageJ 1.50b software

Figure 2. Transverse high-resolution computed tomographic image of the middle thorax in a healthy West Highland white terrier under general anesthesia (A) and using VetMousetrap™ device (B)

84x68mm (300 x 300 DPI)

Figure 2. Transverse high-resolution computed tomographic image of the middle thorax in a healthy West Highland white terrier under general anesthesia (A) and using VetMousetrap™ device (B)

84x68mm (300 x 300 DPI)

Figure 3. Transverse high resolution computed tomography image using VetMousetrap™ device of a dog with canine idiopathic pulmonary fibrosis with severe ground glass opacity

84x69mm (300 x 300 DPI)